Control-Release Polyethylenimine-Modified Fibroin Nanoparticles As A Potential Vehicle for the Oral Delivery of Quercetin

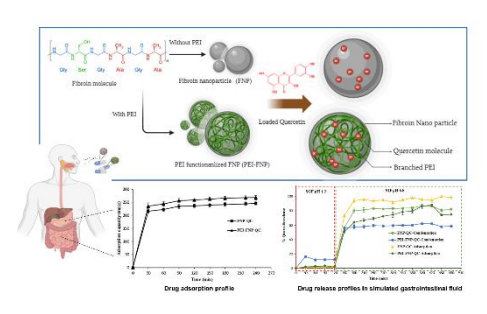
Phuong T.M. Ha¹, Thanh Lich Nguyen², Ngoc Yen Nguyen², Nguyen Trong Tuan², Manh Quan Nguyen³, Tran Thi Bich Quyen⁴, Duy Toan Pham^{2*}

ABSTRACT

Polyphenolic compounds are a big class of chemicals employed in numerous biomedical applications. However, these compounds are susceptible to degradations, especially in the varied gastrointestinal pH, which hinders their use in oral administrations. Thus, this work developed fibroin nanoparticles (FNP) and polyethylenimine-modified FNP (PEI-FNP) to orally protect and deliver quercetin (QC), a model polyphenol. The particles were formulated using two distinct methods: adsorption and co-condensation. Both formulas showed appropriate physicochemical properties for oral administrations, including nano-sizes (~700 nm for FNP-QC and ~200 nm for PEI-FNP-QC), narrow size distribution (polydispersity index < 0.3), adjustable zeta potentials (~-20 mV for FNP-QC and ~+25 mV for PEI-FNP-QC), enhanced QC aqueous solubility to 2-3 times, and observable chemical interactions (hydrogen bonding and ionic interactions) between OC and fibroin/PEI. Moreover, depending on the formulation process and particle compositions, the particles possessed moderate QC entrapment efficiency (35-75%), smooth/rough surfaces, and rapid drug adsorption followed models including Langmuir and Dubinin-Radushkevich isotherms, as well as pseudo-second-order kinetics. Interestingly, in the mimicked oral condition, the particles can protect QC from the gastric condition at pH 1.2, with less than 20% QC release, while sustaining its release in the intestine at pH 6.8, with the release rates that could be favorably controlled by varying the formulation methods and/or PEI functionalization. In summary, the FNP and PEI-FNP demonstrated much potential as release-controllable delivery systems for oral administrations of polyphenolic compounds.

Keywords: Fibroin; Polyethylenimine; Nanoparticles; Quercetin; Oral delivery

GRAPHICAL ABSTRACT



*Corresponding author: Duy Toan Pham

pdtoan@ctu.edu.vn

Received: 01/08/2024 Accepted: 21/09/2024. DOI: https://doi.org/10.35516/jjps.v18i3.3082

¹Department of Chemistry, Faculty of Pharmacy and Nursing, Tay Do University, 68 Tran Chien Street, Can Tho 900000, Vietnam

²Department of Health Sciences, College of Natural Sciences, Can Tho University, Campus II, 3/2 Street, Can Tho 900000, Vietnam

³Department of Analytical Chemistry-Drug Quality Control, Faculty of Pharmacy, Can Tho University of Medicine and Pharmacy, 179 Nguyen Van Cu Street, Can Tho 900000, Vietnam.

⁴Faculty of Chemical Engineering, College of Engineering, Can Tho University, Campus II, 3/2 Street, Can Tho 900000, Vietnam

1. INTRODUCTION

Polyphenolic compounds are bioactive substances prevalent in almost every medicinal plants, possess numerous potential therapeutic efficacies ^{1–3}. Despite their benefits, the effective utilization of polyphenols in oral administration is significantly hampered due to their susceptibility to degradation in varying pH conditions, particularly within the gastrointestinal tract 4. This instability reduces their bioavailability, limiting their therapeutic efficacy when consumed orally. Previous studies have attempted to address these challenges by developing drug delivery systems, namely fibroin micro-/nanoparticles (FNP), to encapsulate, protect, and sustain the release of polyphenols in different plant extracts of guava ⁵ and wedelia ⁶. These research demonstrated that FNP could highly protect these polyphenolic compounds from degradation while preserving their bioactivity. Nevertheless, no research has focused on the FNP ability to orally deliver the polyphenols in the gastrointestinal tract.

To bridge this gap, the current study focuses on the development of FNP, together with its functionalization counterpart, polyethylenimine-modified FNP (PEI-FNP), to encapsulate quercetin (QC), a model polyphenol, for oral application. QC is a popular plant flavonoid found in various vegetables and fruits, which has numerous pharmacological effects, such as reducing inflammatory response (regulating eicosanoids biosynthesis), reducing the low-density liporotein oxidation (preventing atherosclerotic plaque formation), and regulating the enzymatic activities of ornithine carboxylase, calmodulin, or protein kinase ^{7,8}. However, QC application in the pharmaceutical area is constrained by its poor water solubility, low permeability, instability in the gastrointestinal environment, and susceptibility to extensive first-pass metabolism 9-11. Moreover, QC interacts with various dietary components and its stability is influenced by the pH and temperature conditions in the gastrointestinal tract ¹². To this end, drug delivery systems such as liposomes ^{13,14}, lipid-nanocapsules ¹⁵, or inorganic materials such as silica microspheres ^{16,17}, have been explored to improve QC solubility and bioavailability. In this context, proteins have a protective effect and resist degradation of QC, as hydrophobic interactions with proteins are responsible for stabilizing QC ^{18,19}. Thus, protein-based delivery systems such as FNP and PEI-FNP could be a potential approach for QC oral delivery.

Fibroin is the main protein in the silk fiber core, recognized by the US FDA as a biomedical material ^{20,21}. Fibroin has excellent biological properties such as water solubility (in its silk I form) ^{22,23}, slow biodegradation ^{24,25}, non-toxicity and biocompatibility 26-28, making it an outstanding biomaterial. As such, fibroin usages in oral drug delivery has increasingly received a lot of attention ^{29–31}. The unique fibroin structure of anti-parallel amino acid chains with the interactions of intramolecular and intermolecular hydrogen bonds along with van der Waal forces and hydrophobic bonds, providing a stable 3-dimensional structure, thereby increasing fibroin's flexibility, making it stable in a wide pH range and other degrading factors ^{32,33}. Additionally, fibroin has the ability to adhere to mucous membranes 34, making FNP to adhere tightly to intestinal epithelial cells, consequently enhance the encapsulated drug oral bioavailability. At the same time, fibroin degradation in the digestive tract usually takes place slowly (about a few weeks), giving FNP enough time to perform their effects ³⁵. Last but not least, the modification of FNP with PEI, a positively charged polymer commonly used in gene transfer with low cytotoxicity ³⁶, through the ionic interactions, could increase the particle rigidity, drug entrapment efficiency, and controllable release efficiency ^{37,38}.

Ultimately, the main objective of the present work was to focus on the development and usage of FNP and PEI-FNP for the oral delivery of QC. This study aims to fill a significant research gap in the field of polyphenol bioavailability and oral drug delivery systems, providing a novel approach to solve the challenges allied with the gastrointestinal stability and bioavailability of polyphenolic compounds.

2. MATERIALS AND METHODS

2.1. Materials

Cocoons of the *Bombyx mori* silkworm were gathered from Nam Dinh, Vietnam, and fibroin was extracted and purified utilizing the standard process ³⁰. The source of QC and PEI (branched, molecular weight of 25 kDa) was imported from Sigma-Aldrich, Singapore. Ethanol (99.5%) and other chemicals were supplied by general chemical companies and were of at least reagent grade or higher.

2.2. Preparation of the FNP and PEI-FNP

The QC-loaded FNP (FNP-QC) and QC-loaded PEI-FNP (PEI-FNP-QC) were prepared using two different methods: adsorption and co-condensation. For the cocondensation method, 1 mL of the fibroin aqueous solution (8 µg/mL) was mixed with 1 mL ethanol comprising 5 mg OC, without/with 1 mL PEI solution (1% w/v, pH 7.0), to yield the PEI-FNP-QC and FNP-QC, respectively. The mixture was maintained for 24 h at 4°C, cold centrifuged (18,000 rpm, 30 min), and the resulting particles were washed thrice with water. The blank FNP and blank PEI-FNP were also prepared similarly 30. All particles were freeze-dried (-55°C, 72 h) and stored at 4°C for further investigations 38. The free/unencapsulated QC in the centrifuge supernatant was measured by UV-Vis spectroscopy at 370 nm, using a calibration curve (range $0-32 \mu g/mL$, y = 0.0723x - 0.0093, $R^2 = 0.9995$), and the QC entrapment efficiency (EE%) was calculated according to Eq. $(1)^{31}$.

$$EE\% = \frac{5 - Amount of unencapsulated QC (mg)}{5} \times 100 (1)$$

For the adsorption method, the blank FNP or blank PEI-FNP (0.015 g) were dispersed in 50 mL of QC ethanolic solution (100 μ g/mL) for 4 h. To monitor the adsorption process, 1 mL of the dispersion was taken out every 30 min, with medium refilled. The samples were then centrifuged (18,000 rpm, 3 min), and the centrifuge supernatants were UV-Vis spectroscopic analyzed at 370

nm to evaluate the unadsorbed QC. The QC adsorption efficiency (%) was calculated according to **Eq. (2)**, where Ce is the QC equilibrium concentration (μ g/mL).

QC adsorption efficiency (%) =
$$\frac{100 - C_e}{100} \times 100$$
 (2)

2.3. Characterizations of the FNP and PEI-FNP

Particle size, polydispersity index, and zeta potential

The mean particle size, size distribution (polydispersity index, PI), and zeta potentials were measured by the dynamic light scattering (DLS) and phase analysis light scattering (PALS) technique, respectively, using ZetaPALS® analyzer (Brookhaven Instrument Corporation, USA) installed with a helium-neon laser diode (35 mW, 632.8 nm). The particles were diluted with water until a count rate of 500-600 kcps, and the measurements were conducted in triplicate at 25°C.

Particles morphology

Scanning electron microscope (SEM, Carl Zeiss, Germany) was utilized to illustrate the particle morphology. The particles were re-dispersed in water and diluted until a count rate of 400 kcps and the dispersions were dropwise added onto 100-nm plastic discs, which were mounted on a metal base, followed by gold coating, and observed by SEM.

Particles structure

The particle structures and chemical interactions were determined using Fourier-transform infrared spectroscopy (FT-IR, Jasco 6300, Japan), using the KBr tablet technique. The spectra were acquired in a 4000-400 cm⁻¹ wavenumber range at a resolution of 4.0 cm⁻¹.

Drug solubility

The aqueous solubility of the free/pure QC, QC in FNP-QC, and QC in PEI-FNP-QC, was tested in phosphate buffer saline (PBS). The samples were dispersed in PBS, stirred overnight (200 rpm, 25°C), cold centrifuged (18,000 rpm, 30 min), and the supernatant was UV-Vis measured at 376.5 nm. The QC solubility was determined as the highest concentration of QC in PBS,

with a QC standard curve in PBS (y = 0.0684x - 0.0037, $R^2 = 0.9993$).

2.4. Isotherm and kinetics of QC adsorption

The QC adsorption process onto the FNP and PEI-FNP was evaluated utilizing the standard isothermal and kinetics models. The Langmuir model (Eq. (3)) describes whether the adsorption process is monolayer or multilayers. The Freundlich model describes a physical type of adsorption occurring in multilayer, with the assumption that the adsorption sites are heterogeneous (Eq. (4)). The Dubinin-Radushkevich model (Eq. (5)) assesses the adsorption nature of physical or chemical adsorption. The pseudo-first-order kinetics (Eq. (6)) and pseudo-second-order kinetics (Eq. (7)) show the adsorption rates and properties of the QC onto the particles.

$$\frac{q_e}{q_m} = \frac{K_L C_e}{1 + K_L C_e} \quad (3)$$

$$q_e = K_F C_e^{1/n}$$
 (4)

$$lnq_e = lnq_m - \beta \epsilon^2$$
 (5)

$$ln(q_e - q_t) = ln(q_e) - k_1 t$$
 (6)

$$\frac{t}{q_t} = \frac{1}{k_2 q_e^2} + \frac{t}{q_e}$$
 (7)

where q_e , q_m , q_t are the QC equilibrium adsorption capacity, the maximum adsorption capacity, and the adsorption capacity at time point t (mg/g), respectively; C_e is the FNP/PEI-FNP concentration (mg/L); β is the adsorption energy constant; K_L is the Langmuir constant; K_F is the Freundlich constant; n is the number demonstrating the degree of linearity between the adsorbate and the adsorption process; ϵ is the Polanyi potential energy; k_1 and k_2 are the pseudo-first-order and pseudo-second-order kinetics rate constant.

2.5. In-vitro QC release in simulated oral condition

The FNP-QC and PEI-FNP-QC were evaluated for

their ability to release QC at 37°C in the mimicked gastrointestinal condition, utilizing the standard shaking method. Firstly, the FNP-QC and PEI-FNP-QC were dispersed in 10 mL HCl (pH 1.2), which simulates gastrointestinal juice, for 2 h. Then, the FNP-QC/PEI-FNP-QC were subjected to 40 mL PBS (pH 6.8), which simulates intestinal fluid, for an additional 6 h. Every 30 min, 1 mL dispersion was taken out, with medium refilled, centrifuged at 18,000 rpm for 3 min, and the OC released was measured by UV-Vis spectroscopy method. The absorbance was determined at 368.5 nm in the HCl medium (y = 0.0553x - 0.0048, $R^2 = 0.9985$, range 0-10 μ g/mL), and at 376.5 nm in the PBS medium (y = 0.0684x -0.0037, $R^2 = 0.9993$, range 0-10 µg/mL). The QC release (%) was determined by Eq. (8), with C_t and C_i are the released QC concentrations at the time t and i, Vo is the total medium volume, Mo and Mi are the QC initial and the QC withdrawal amount at the time i.

QC release (%) =
$$\frac{C_t V_0 + \sum_{i=1}^{t-1} C_i}{M_0 - \sum_{i=1}^{t-1} M_i} \times 100$$
 (8)

3. RESULTS AND DISCUSSIONS

3.1 Preparation of the FNP and PEI-FNP

In this study, the FNP-QC and PEI-FNP-QC were formulated using the simple one-pot preparations employing the co-condensation or adsorption technique. Then, all particles were characterized in terms of sizes, PI, zeta potentials, morphology, chemical interactions, and QC solubility. Finally, the in-vitro QC release profiles in the oral simulated condition were investigated. The particles were successfully prepared and characterized, discussed in the next sections.

3.2. Characterizations of the FNP and PEI-FNP

Firstly, both the blank and QC-loaded particles were successfully prepared with nano-sized (150-700 nm) and narrow size distribution (PI < 0.3) (**Table 1**). The PEI-FNP showed statistically smaller sizes than those of the FNP, which was due to the tightening and rigidifying effects based on ionic interactions between the PEI (positive

charge) and the fibroin molecules (negative charge), in agreements with previous studies ^{30,38}. When being loaded with QC, the particles sizes increased, possibly due to additional interactions (i.e., hydrophobic interactions, hydrogen bonding, and ionic interactions) between the QC and fibroin/PEI, consequently enlarging the particles ⁶. These interactions are discussed in the FT-IR section.

Secondly, the zeta potentials of PEI-FNP shifted to positive values, indicating the presence of PEI, whereas the FNP showed negative values of the fibroin inherent negative charge. This fact expands the versatility of FNP in biomedical applications ^{38,39}. Moreover, the incorporation of QC into the particulate systems slightly reduced the zeta potentials to a more negative value (i.e., from -15 mV of blank FNP to -22 mV of FNP-QC; from +33 mV of blank PEI-FNP to +26 mV of PEI-FNP-QC). This was because the QC has five pKa of 7.17, 8.26, 10.13, 12,30, and 13.11 ⁴⁰, making QC mostly stays in the anionic form at neutral pH, consequently shifted the system zeta potentials to be more negative.

Table 1. Particle size, PI, zeta potential, and QC EE% of the FNP-QC and PEI-FNP-QC, together with the blank counterparts (n = 3).

Formula	Size (nm)	PI	Zeta potential (mV)	QC entrapment efficiency (%)	
				Co-condensation	Adsorption
Blank FNP	328.1 ± 13.4	0.16 ± 0.02	-15.5 ± 1.1	-	-
Blank PEI-FNP	176.2 ± 10.2	0.11 ± 0.03	$+33.7 \pm 2.4$	-	-
FNP-QC	680.4 ± 24.7	0.12 ± 0.02	-22.7 ± 1.2	35.8 ± 2.6	67.9 ± 2.2
PEI-FNP-QC	219.8 ± 20.3	0.13 ± 0.02	$+26.7 \pm 2.9$	55.9 ± 5.3	75.5 ± 2.9

Regarding the QC EE%, in the preliminary experiments, the initial QC loading amounts were varied (1 mg, 5 mg, and 10 mg) in both formulation methods. The results showed that at high OC amount of 10 mg, the particles were unstable, easy to aggregate to from micron-size clumps, whereas at lower OC amounts of 1 mg and 5 mg, the nanoparticles were achieved. Moreover, no significant differences were noted between the formulas with 1 mg and 5 mg QC. Thus, to maximize the drug loading amount, we selected the initial QC amount of 5 mg. Both cocondensation and adsorption techniques yielded a moderate EE% of 30-70%, depending on the entrapment method (Table 1). It was found that the adsorption method had a higher EE% than that of the co-condensation method for both formulations. This was due to disparities in drug molecule behaviors concerning the two methods. Regarding the co-condensation technique, the drug molecules dissolved in ethanol were co-condensed with fibroin during the particle formation 41, consequently, the QC molecules were encapsulated in the particle mainly in the crystalline form (proven in the SEM images, with the QC crystals presented on the particle surfaces (Figure 1)). Due to the moderate solubility of QC in ethanol (4 mg/mL at 37°C ⁴²), a part of the drug molecules stayed in the amorphous form and was not co-precipitated, thereby reducing the OC EE%. Besides, in the adsorption process, all drug molecules (100%) were in molecular form and can freely interact with FNP and PEI-FNP. As a consequence, more QC could be adsorbed and absorbed onto and into the particles in its amorphous form, thus increasing the EE% 30. Interestingly, the PEI-FNP provided higher OC EE% than that of FNP for both adsorption and co-condensation methods. This was because of the additional ionic interactions between the PEI (positive charge) and QC (negative charge), which make more OC molecules being encapsulated into the particles ^{38,43}. On the other hand, both the fibroin and QC had negative charges, thus the repulsion forces decreased the EE% of the FNP-QC formula.

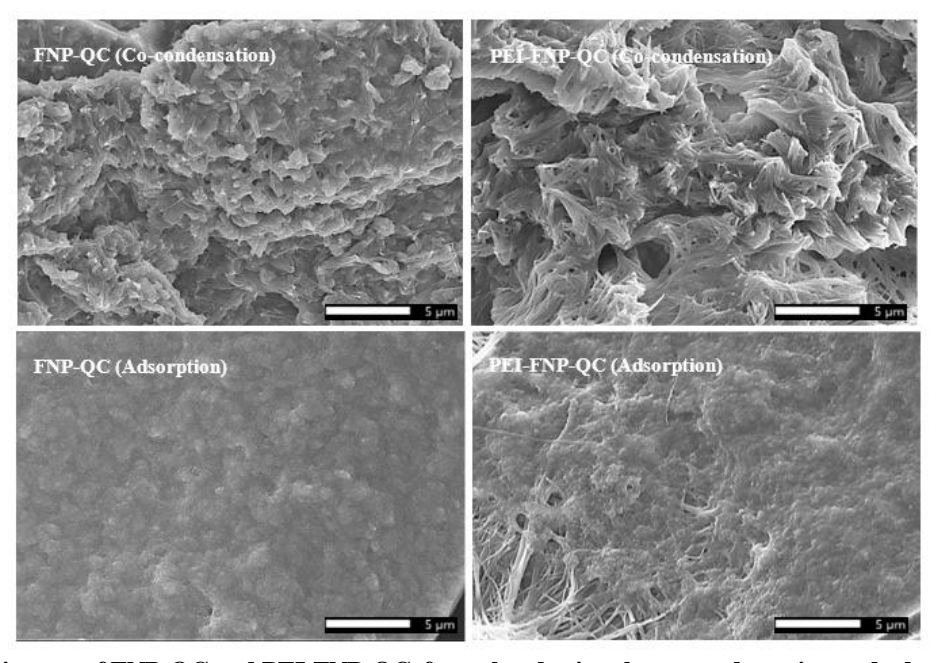


Figure 1. SEM images of FNP-QC and PEI-FNP-QC, formulated using the co-condensation and adsorption techniques.

In terms of the particle morphology, the SEM micrographs showed distinct patterns between the particles formulated by the adsorption method and the cocondensation method (**Figure 1**). As previously discussed, in the co-condensation process, the QC was precipitated on the particle surfaces, making their crystals visually appeared in the images. On the other hand, the FNP-QC and PEI-FNP-QC made by the adsorption technique demonstrated a uniform distribution of spherical particles, linked together into large arrays to create a complete nanoparticle system on which QC molecules are attached in amorphous form. This result was consistent with that of previous studies 44-46.

To elucidate the particle structures and chemical interactions, the FT-IR spectroscopy was employed (**Figure 2**). The blank FNP and PEI-FNP show the silk-II water-insoluble fibroin structure with distinguished peaks of the amide I, II, and III structures, at 1626 cm⁻¹ (C=O stretch signals), 1525 cm⁻¹ (N-H bending signals), and 1234 cm⁻¹ (C-N stretch signals), indicating the success formulation process ³⁸. The PEI-FNP shows PEI

characterized peak at ~2900 cm⁻¹ (PEI C-H stretch), suggesting the PEI was incorporated into the FNP structure. Moreover, after encapsulating the OC, both FNP-QC and PEI-FNP-QC demonstrate QC distinctive peaks at 1666 cm⁻¹ (C=O stretching vibration), 3406 or 3283 cm⁻¹ (-OH stretching vibration), and at 1610, 1560, 1510 cm⁻¹ (C=C stretching signals of the aromatic rings), indicating that the QC molecules were successfully loaded into the nanoparticle systems. Interestingly, the intensities of the amide I and amide III peaks of the FNP-QC and PEI-FNP-QC were reduced, compared to those of the blank counterparts, suggesting that the QC formed additional bonding with fibroin at these two locations, possibly the hydrogen bonding between oxygen and nitrogen atoms of fibroin with the hydrogen atoms of QC. Furthermore, the PEI signal of PEI-FNP-QC was also decreased, confirming the ionic interaction between negatively charged QC and positively charged PEI. Overall, these chemical interactions were in well agreement with the particles properties, as previously discussed.

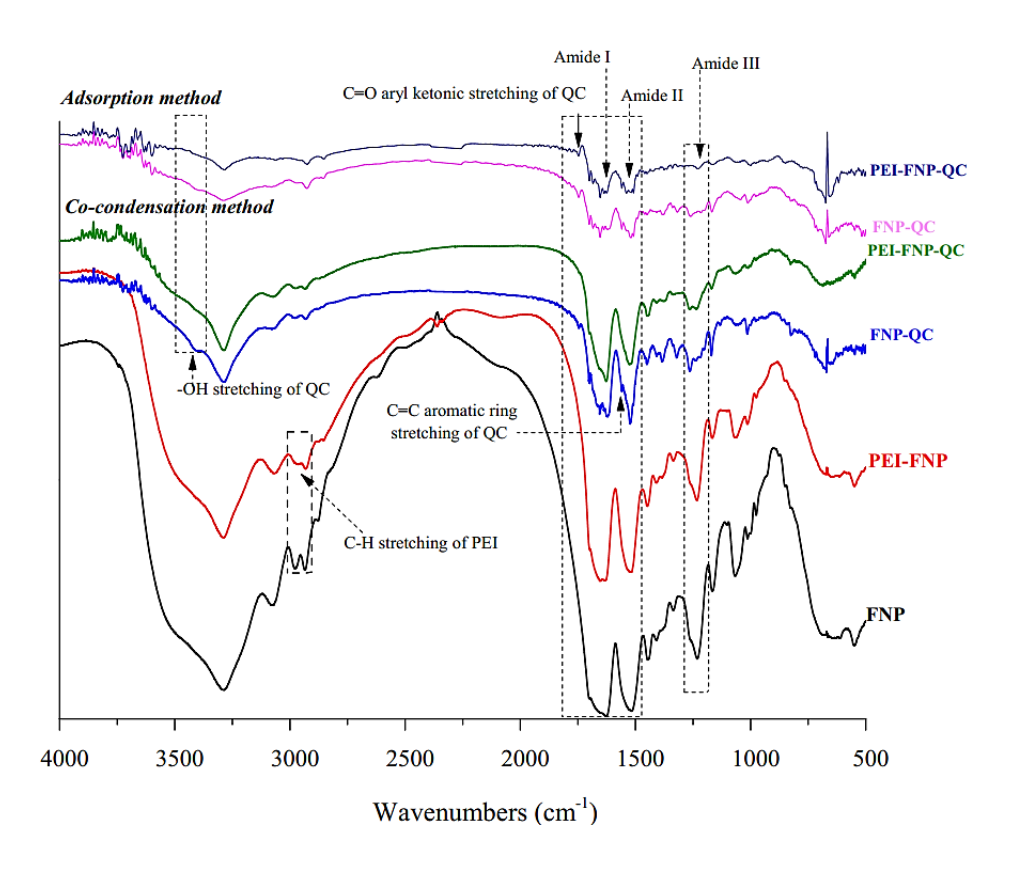


Figure 2. FT-IR spectra of the blank FNP, blank PEI-FNP, FNP-QC, and PEI-FNP-QC, formulated using the co-condensation and adsorption techniques.

For the QC water solubility test, the pure QC has very low aqueous solubility of $29.7 \pm 1.2~\mu g/mL$. Remarkably, owning to the submicron sizes, both FNP-QC and PEI-FNP-QC statistically increased the QC solubility by 2-3 times, following the order of pure QC $(29.7 \pm 1.2~\mu g/mL)$ < FNP-QC-Co-condensation $(48.2 \pm 2.3~\mu g/mL)$ < PEI-FNP-QC-Co-condensation $(62.7 \pm 4.7~\mu g/mL)$ < FNP-QC-Adsorption $(73.1 \pm 5.5~\mu g/mL)$ < PEI-FNP-QC-Adsorption $(89.4 \pm 6.2~\mu g/mL)$. The fact that the adsorption technique produced particles with greater QC solubility than those of the co-condensation technique was attributed to the QC polymorphs, of which the QC mainly stayed in crystalline form in co-condensation-particles and in amorphous form in adsorption-particles. This phenomenon was proven by the SEM images (**Figure 1**)

and in well agreement with the previous published report ³⁰. Thus, the QC in co-condensation-particles encountered more difficult to be dissolved in water. Additionally, the solubility of PEI-FNP-QC was significantly higher than that of FNP-QC, which was because PEI molecules act as a surfactant, thereby helping to solubilize the QC ³⁰.

Overall, the FNP-QC and PEI-FNP-QC were successfully formulated with appropriate properties that are beneficial for the oral administration.

3.3. Isotherm and kinetics of QC adsorption

The QC adsorption capacity over time of both the FNP and PEI-FNP is presented in **Figure 3**. The adsorption process was divided into two main stages of the rapid adsorption within 30 min, followed by a steadily-increase adsorption stage until 4 h. The PEI-FNP exhibited greater

adsorption capacities than the FNP, which reflected the complementary ionic interactions of PEI and QC, thereby enhancing the amount of drug bound on the particles.

To elucidate the mechanism of the QC adsorption process, the study described the standard isotherm (Langmuir, Freundlich, and Dubinin-Radushkevich 47 and kinetics models (pseudo-first-order and pseudo-secondorder). Both FNP and PEI-FNP did not followed the Freundlich model ($R^2 < 0.9$) and followed well with the Langmuir and Dubinin-Radushkevich model, with R² > 0.9 for all formulas (**Figure 4**). This fact indicates that the QC adsorption on the particles might not be governed by multilayer process on heterogeneous surfaces. Based on the Langmuir model, we determined the highest theoretical adsorption capacity of this process was 158.7 mg/g for FNP and 192.3 mg/g for PEI-FNP. In fact, the experimental adsorption capacity of this process was ~210 mg/g for FNP and ~230 mg/g for PEI-FNP. This suggests that the QC adsorption process was mainly monolayer, with some extra interactions between the QC and fibroin/PEI molecules, possibly through the van der Waals force and hydrogen interactions 30 . Further research are necessary to elucidate this issue. Besides, with the energy of the adsorption process (E) calculated based on the Dubinin-Radushkevich model (E = $1/\sqrt{2\beta}$) of 0.036 kJ/mol (< 8 kJ/mol) for FNP-QC and 0.033 kJ/mol (< 8 kJ/mol) for PEI-FNP-QC, it can be concluded that the nature of the adsorption process of QC onto FNP and PEI-FNP particles was mainly a physical adsorption process. This was in accordance with the FT-IR results, since most of the interactions between QC and fibroin/PEI was hydrogen bonding and ionic interactions.

Regarding the adsorption kinetics, the adsorption process of QC onto FNP and PEI-FNP particles in this study was mainly followed the pseudo-second-order kinetics model with $R^2 = 0.9998$ for FNP-QC and $R^2 = 0.9999$ for PEI-FNP-QC, instead the pseudo-first-order kinetics model with lower R^2 of 0.9744 for FNP-QC and 0.9138 for PEI-FNP-QC (**Figure 4**). This fact suggests that both FNP and PEI-FNP demonstrate rapid adsorption rates.

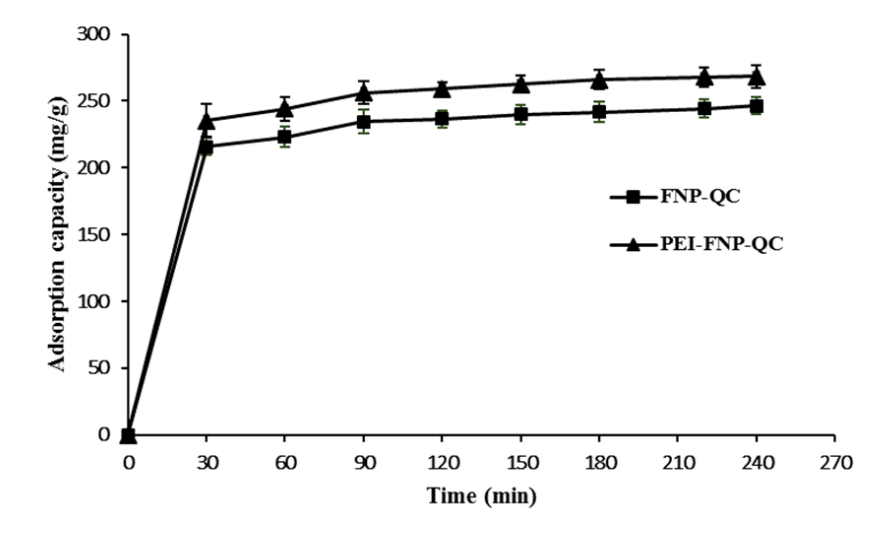


Figure 3. Adsorption capacity (mg/g) of QC on the FNP and PEI-FNP (n = 3). The adsorption process was conducted with 0.015 g of blank FNP or blank PEI-FNP, dispersed in 50 mL of QC ethanolic solution (100 μ g/mL) for 4 h at 25°C.

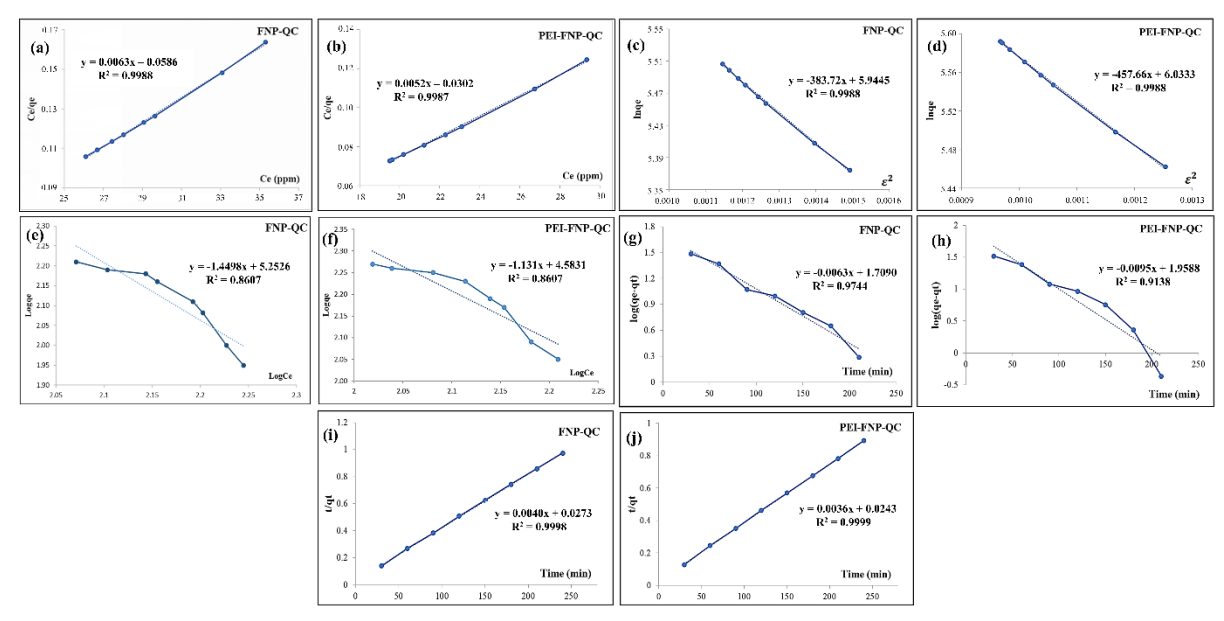


Figure 4. Adsorption isotherms (Langmuir (a, b), Dubinin-Radushkevich (c, d), and Freundlich (e, f)) and kinetics (pseudo-first-order (g, h), pseudo-second-order (i, j)) model fitting of QC on the FNP and PEI-FNP.

3.4. In-vitro OC release in simulated oral condition

To evaluate the in-vitro release processes of QC from FNP-QC and PEI-FNP-QC, the experiments were performed under conditions simulating the human gastrointestinal tract, with HCl pH 1.2 for 2 h and PBS pH 6.8 for the subsequent 6 h (**Figure 5**). In general, the QC release was limited to less than 20% QC released in the gastric juice environment for both FNP-QC and PEI-FNP-QC particles formulated by both adsorption and cocondensation technique. This result demonstrated the ability of FNP and PEI-FNP particles to protect QC in the critical gastric environment in human body. This was because both fibroin and PEI possess many different amino groups acting as basic buffer systems, thereby neutralizing the acidic micro-environment surrounding the particles ³⁸.

During the next 6-h, under simulated intestinal conditions at pH 6.8, the QC release pattern differed between the two encapsulation methods. Roughly, the pattern followed the order of FNP-QC-Adsorption > FNP-QC-Co-condensation > PEI-FNP-QC-Adsorption > PEI-FNP-QC-Adsorp

FNP-QC-Co-condensation. As such, the adsorption-particles released faster than the co-condensation-particles, and the PEI-modified particles released slower than the non-modified particles. Expectedly, as previously discussed in **section 3.2**, the co-condensation particles had most of QC molecules presented in crystalline form, with limited solubility, therefore, the QC was released slower than those of the adsorption method, which possessed QC amorphous form and higher solubility. Moreover, **section 3.3** also proves that most QC was adsorbed onto the FNP and PEI-FNP particles through a physical adsorption process, with deficient interactions and small adsorption energy. Thus, the desorption process was simple and rapid⁴⁸.

Interestingly, although the PEI-FNP-QC demonstrated higher QC solubility than those of FNP-QC, the release results of PEI-FNP-QC showed slower release efficiency than FNP-QC particles. This fact could be explained by two reasons. Firstly, as discussed in the FT-IR section, the PEI-FNP-QC form additional ionic interactions between PEI and QC, making it more difficult for the QC molecules

to be dissolved out into the buffer. Secondly, the PEI-FNP-QC particle sizes were small, with compact and tight structure ³⁸, thus, the buffer water molecules could not freely come into contact with QC molecules in the particle cores, consequently limiting the solvating process and reducing the QC released amount.

Notably, during the whole release process, there is a slight fluctuation in the percentages of the released QC, which might be due to a part of the released QC molecules

being hydrolyzed in the medium, leading to a minor decrease in total QC amounts.

In summary, the particles could protect QC from the gastric condition, while facilitating its release in the intestinal condition, which was favorable for oral administration. More importantly, one can precisely control the release rate of QC by adjusting the formulation methods (i.e., co-condensation and adsorption) and/or the PEI functionalization.

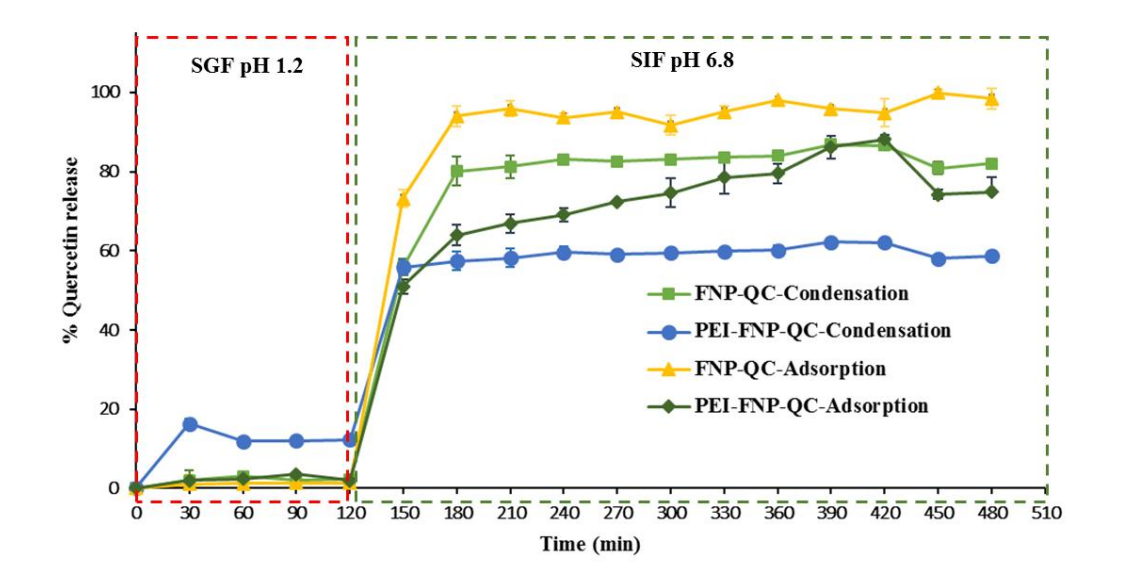


Figure 5. The release profiles of QC in simulated gastrointestinal fluid (pH 1.2 for 2 h and pH 6.8 for the next 6 h) at 37°C of FNP-QC and PEI-FNP-QC, formulated using co-condensation and adsorption techniques (n = 3).

4. CONCLUSIONS

This study prepared FNP and PEI-FNP for QC oral delivery using two techniques: adsorption and cocondensation. The formulas demonstrated appropriate physicochemical properties for oral administrations, including nano-sizes, narrow size distribution, adjustable zeta potentials, moderate QC encapsulation, smooth/rough surfaces dependent on the formulation process, observable chemical interactions, and increased drug solubility. In the simulated oral condition, the particles could protect QC from the gastric condition at pH 1.2, with less than 20%

QC release, while facilitating its release in the intestinal condition. Lastly but most importantly, the fast/slow/sustain release rates of QC could be favorably controlled and adjusted by varying the formulation methods and/or PEI functionalization. The study has some limitations, including (1) the study primarily focuses on invitro conditions, which may not fully predict in-vivo behavior due to the complexity of biological systems, and (2) the use of PEI, while beneficial for modifying nanoparticle properties, could raise concerns about cytotoxicity and biocompatibility, which needs thorough

evaluation. Future research should focus on the in-vivo studies to assess the bioavailability, pharmacokinetics, and overall efficacy of FNP-QC and PEI-FNP-QC, the long-term stability of the particles, and the toxicity and safety evaluations. In conclusion, the FNP and PEI-FNP are potential delivery systems for oral administrations, with adjustable release properties, and could open new avenues for oral delivery of bioactive molecules.

Statements and Declarations

Acknowledgements

The authors acknowledge Tay Do University, Can Tho University of Medicine and Pharmacy, and Can Tho University for the supports.

Funding

None.

REFERENCES

- Pietta P, Minoggio M, Bramati L. Plant Polyphenols: Structure, Occurrence and Bioactivity. In: *Studies in Natural Products Chemistry*. (Rahman A. ed). Bioactive Natural Products (Part I) Elsevier; 2003; pp. 257–312; doi: 10.1016/S1572-5995(03)80143-6.
- Pandey KB, Rizvi SI. Plant polyphenols as dietary antioxidants in human health and disease. *Oxid Med Cell Longev*. 2009;2(5):270–278.
- Huynh DTM, Le M-NT, Tran VD, et al. Native Medicinal Plants (Moringa oleifera Lam, Brucea javanica (L.) Merr., Eclipta prostrata (L.), Callisia fragrans (Lindl.) Woodson, and Zingiber zerumbet (L.) Smith) in An Giang, Vietnam: A Preliminary Investigation for Rhabdomyosarcoma Treatments using in-vitro RD cell cytotoxicity test. *Jordan Journal of Pharmaceutical Sciences*. 2023;16(4):830–841; doi: 10.35516/jips.v16i4.1365.
- 4. Friedman M, Jürgens HS. Effect of pH on the Stability of Plant Phenolic Compounds. *J Agric Food Chem*. 2000;48(6):2101–2110; doi: 10.1021/jf990489j.

Competing interests

The authors have no competing interests to declare that are relevant to the content of this article.

Data availabity

The data that support the findings of this study are available from the corresponding author, Duy Toan Pham, upon reasonable request.

Author contributions

Conceptualization: P.T.M.H., D.T.P.; methodology: P.T.M.H., T.L.N., N.Y.N., N.T.T., M.Q.N., T.T.B.Q., D.T.P.; investigation: P.T.M.H., T.L.N., N.Y.N., N.T.T., M.Q.N., T.T.B.Q.; data curation: P.T.M.H., D.T.P.; validation: D.T.P.; project administration: D.T.P.; resource: D.T.P.; writing-original draft: P.T.M.H., D.T.P.; writing-review and editing: P.T.M.H., T.L.N., N.Y.N., N.T.T., M.Q.N., T.T.B.Q., D.T.P.

- Pham DT, Nguyen DXT, Lieu R, et al. Silk nanoparticles for the protection and delivery of guava leaf (Psidium guajava L.) extract for cosmetic industry, a new approach for an old herb. *Drug Delivery*. 2023;30(1):2168793; doi: 10.1080/10717544.2023.2168793.
- Pham DT, Huynh QC, Lieu R, et al. Controlled-Release Wedelia trilobata L. Flower Extract Loaded Fibroin Microparticles as Potential Anti-Aging Preparations for Cosmetic Trade Commercialization. *Clinical, Cosmetic* and Investigational Dermatology. 2023;16:1109–1121; doi: 10.2147/CCID.S405464.
- Anand David AV, Arulmoli R, Parasuraman S. Overviews of Biological Importance of Quercetin: A Bioactive Flavonoid. *Pharmacogn Rev.* 2016;10(20):84– 89; doi: 10.4103/0973-7847.194044.

- 8. Alshieka M, Jandali R, Agha MIH. A Comparative Study of in Vitro Lipoxygenase Inhibition and DPPH (1, 1-Diphenyl-2-Picrylhydrazyl) Free Radical Scavenging Activity of Silybum marianum and [Notobasis syriaca (L.) Cass.] Fruits and Linum usitatisimum Seeds. *Jordan Journal of Pharmaceutical Sciences*. 2023;16(2):561–561; doi: 10.35516/jjps.v16i2.1500.
- Atul Bhattaram V, Graefe U, Kohlert C, et al. Pharmacokinetics and bioavailability of herbal medicinal products. *Phytomedicine: international journal of* phytotherapy and phytopharmacology. 2002;9 Suppl 3(SUPPL. 3):1–33; doi: 10.1078/1433-187X-00210.
- Fasolo D, Schwingel L, Holzschuh M, et al. Validation of an isocratic LC method for determination of quercetin and methylquercetin in topical nanoemulsions. *Journal of Pharmaceutical and Biomedical Analysis*. 2007;44(5):1174–1177; doi: 10.1016/J.JPBA.2007.04.026.
- Kumari A, Yadav SK, Pakade YB, et al. Development of biodegradable nanoparticles for delivery of quercetin. *Colloids and surfaces B, Biointerfaces*. 2010;80(2):184– 192; doi: 10.1016/J.COLSURFB.2010.06.002.
- 12. Bordenave N, Hamaker BR, Ferruzzi MG. Nature and consequences of non-covalent interactions between flavonoids and macronutrients in foods. *Food & function*. 2014;5(1):18–34; doi: 10.1039/C3FO60263J.
- 13. Priprem A, Watanatorn J, Sutthiparinyanont S, et al. Anxiety and cognitive effects of quercetin liposomes in rats. *Nanomedicine: nanotechnology, biology, and medicine*. 2008;4(1):70–78; doi: 10.1016/J.NANO.2007.12.001.
- Mignet N, Seguin J, Chabot GG. Bioavailability of polyphenol liposomes: a challenge ahead. *Pharmaceutics*. 2013;5(3):457–471; doi: 10.3390/PHARMACEUTICS5030457.
- Russo M, Spagnuolo C, Tedesco I, et al. The flavonoid quercetin in disease prevention and therapy: facts and fancies. *Biochemical pharmacology*. 2012;83(1):6–15; doi: 10.1016/J.BCP.2011.08.010.

- 16. Kim YH, Lee DW, Jung EJ, et al. Preparation and characterization of quercetin-loaded silica microspheres stabilized by combined multiple emulsion and sol-gel processes. *Chemical Industry and Chemical Engineering Quarterly*. 2015;21(1–1):85–94; doi: 10.2298/CICEQ131002010K.
- 17. Ibraheem LM, Khattabi AM. Studying the Effect of Functional Group and Size of Silica Nanoparticles Loaded with Quercetin on their in vitro Characteristics. *Jordan Journal of Pharmaceutical Sciences*. 2022;15(4):569–582; doi: 10.35516/jips.v15i4.679.
- Desai KGH, Park HJ. Recent Developments in Microencapsulation of Food Ingredients. *Drying Technology*. 2005;23(7):1361–1394; doi: 10.1081/DRT-200063478.
- Wang J, Zhao XiH. Degradation kinetics of fisetin and quercetin in solutions affected by medium pH, temperature and co-existed proteins. *Journal of the Serbian Chemical Society*. 2016;81(3):243–253; doi: 10.2298/JSC150706092W.
- 20. Pham DT, Thao NTP, Thuy BTP, et al. Silk fibroin hydrogel containing Sesbania sesban L. extract for rheumatoid arthritis treatment. *Drug delivery*. 2022;29(1):882–888; doi: 10.1080/10717544.2022.2050848.
- 21. Pham DT, Tiyaboonchai W. Fibroin nanoparticles: a promising drug delivery system. *Drug delivery*. 2020;27(1):431–448; doi: 10.1080/10717544.2020.1736208.
- 22. Valluzzi R, Gido S. *Orientation of Silk III at the Air Water Interface*. n.d.
- 23. Wongpinyochit T, Johnston BF, Seib P. *Degrradation Behavior of Silk Nanoparticles Enzyme Responiveness*.
 n.d.
- 24. Farokhi M, Mottaghitalab F. Sustained Release of Platelet-Deried Growth Factor and Vascular Endothelial Growth Factor from Silk/Calcium Phosphate/PLGA Based Nanocomposite Scafold. *Internation Journal of Pharmaceutics*. 2013;454:216-225.

- Numata K, Cebe P, Kaplan DL. Mechanism of Enzymatic Degradation of Beta-Sheet Crystals. *Biomaterials*. 2010;31(10):2926–2933; doi: 10.1016/j.biomaterials.2009.12.026.
- 26. Sakabe H, Ito H, Miyamonto T. In *Vivo Compatibility of Regenerated Fibroin*. 1989;45(11):487–490.
- 27. Santin M, Motta A, Freddi G, et al. In Vitro Evaluation of the Inflammatory Potential of the Silk Fibroin. *Journal of Biomedical Materials Research*. 1999;46(3):382–389; doi: 10.1002/(SICI)1097-4636(19990905)46:3<382::AID-JBM11>3.0.CO;2-R.
- 28. Konishi T, Kurokawa M. The Structure of Silk Fibroin-α. *Sen'i Gakkaishi*. 1968;24(12):550–554; doi: 10.2115/fiber.24.550.
- 29. Crivelli B, Bari E, Perteghella S, et al. Silk fibroin nanoparticles for celecoxib and curcumin delivery: ROS-scavenging and anti-inflammatory activities in an in vitro model of osteoarthritis. European journal of pharmaceutics and biopharmaceutics: official journal of Arbeitsgemeinschaft fur Pharmazeutische Verfahrenstechnik eV. 2019;137:37–45; doi: 10.1016/j.ejpb.2019.02.008.
- 30. Pham DT, Nguyen TL, Nguyen TTL, et al. Polyethylenimine-functionalized fibroin nanoparticles as a potential oral delivery system for BCS class-IV drugs, a case study of furosemide. *Journal of Materials Science*. 2023;58(23):9660–9674; doi: 10.1007/S10853-023-08640-Y/METRICS.
- Pham DT, Saelim N, Tiyaboonchai W. Alpha mangostin loaded crosslinked silk fibroin-based nanoparticles for cancer chemotherapy. *Colloids and surfaces B, Biointerfaces*. 2019;181:705–713; doi: 10.1016/J.COLSURFB.2019.06.011.
- 32. Ki CS, Park YH, Jin HJ. Silk protein as a fascinating biomedical polymer: Structural fundamentals and applications. *Macromolecular Research*. 2009 17:12 2009;17(12):935–942; doi: 10.1007/BF03218639.

- 33. Keten S, Xu Z, Ihle B, et al. Nanoconfinement controls stiffness, strength and mechanical toughness of beta-sheet crystals in silk. *Nature materials*. 2010;9(4):359–367; doi: 10.1038/NMAT2704.
- 34. Brooks AE. The Potential of Silk and Silk-Like Proteins as Natural Mucoadhesive Biopolymers for Controlled Drug Delivery. Frontiers in chemistry. 2015;3(NOV); doi: 10.3389/FCHEM.2015.00065.
- Koperska MA, Pawcenis D, Milczarek JM, et al. Fibroin degradation Critical evaluation of conventional analytical methods. *Polymer Degradation and Stability*. 2015;120:357–367; doi: 10.1016/J.POLYMDEGRADSTAB.2015.07.006.
- 36. Goula D, Benoist C, Mantero S, et al. Polyethylenimine-based intravenous delivery of transgenes to mouse lung. *Gene therapy*. 1998;5(9):1291–1295; doi: 10.1038/SJ.GT.3300717.
- 37. Pham DT, Saelim N, Cornu R, et al. Crosslinked Fibroin Nanoparticles: Investigations on Biostability, Cytotoxicity, and Cellular Internalization. *Pharmaceuticals*. 2020;13(5); doi: 10.3390/PH13050086.
- Pham DT, Saelim N, Tiyaboonchai W. Crosslinked fibroin nanoparticles using EDC or PEI for drug delivery: physicochemical properties, crystallinity and structure. *Journal of Materials Science*. 2018 53:20 2018;53(20):14087–14103; doi: 10.1007/S10853-018-2635-3.
- 39. Pham DT, Tetyczka C, Hartl S, et al. Comprehensive investigations of fibroin and poly(ethylenimine) functionalized fibroin nanoparticles for ulcerative colitis treatment. *Journal of Drug Delivery Science and Technology*. 2020;57:101484; doi: 10.1016/J.JDDST.2019.101484.
- 40. PubChem. Quercetin. n.d. Available from: https://pubchem.ncbi.nlm.nih.gov/compound/5280343 [Last accessed: 7/18/2024].

- Pham DT, Nguyen DXT, Nguyen NY, et al. Development of pH-responsive Eudragit S100-functionalized silk fibroin nanoparticles as a prospective drug delivery system. *PLOS ONE*. 2024;19(5):e0303177; doi: 10.1371/journal.pone.0303177.
- 42. Wang W, Sun C, Mao L, et al. The biological activities, chemical stability, metabolism and delivery systems of quercetin: A review. *Trends in Food Science & Technology*. 2016;56:21–38; doi: 10.1016/J.TIFS.2016.07.004.
- 43. Bayraktar O, Malay Ö, Özgarip Y, et al. Silk fibroin as a novel coating material for controlled release of theophylline. European journal of pharmaceutics and biopharmaceutics: official journal of Arbeitsgemeinschaft fur Pharmazeutische Verfahrenstechnik eV. 2005;60(3):373–381; doi: 10.1016/J.EJPB.2005.02.002.
- 44. Zhan S, Paik A, Onyeabor F, et al. Oral Bioavailability Evaluation of Celastrol-Encapsulated Silk Fibroin Nanoparticles Using an Optimized LC-MS/MS Method. *Molecules (Basel, Switzerland)*. 2020;25(15); doi: 10.3390/MOLECULES25153422.

- 45. Khosropanah MH, Vaghasloo MA, Shakibaei M, et al. Biomedical applications of silkworm (Bombyx Mori) proteins in regenerative medicine (a narrative review). *Journal of tissue engineering and regenerative medicine*. 2022;16(2):91–109; doi: 10.1002/TERM.3267.
- 46. Dong JW, Cai L, Xing Y, et al. Re-evaluation of ABTS*+ Assay for Total Antioxidant Capacity of Natural Products. *Natural product communications*. 2015;10(12):2169–2172; doi: 10.1177/1934578x1501001239.
- 47. Chen L, Jiang Z, Liu K, et al. Application of Langmuir and Dubinin–Radushkevich models to estimate methane sorption capacity on two shale samples from the Upper Triassic Chang 7 Member in the southeastern Ordos Basin, China. *Energy Exploration & Exploitation*. 2017;35(1):122–144; doi: 10.1177/0144598716684309.
- 48. Nguyen NNT, Pham DT, Nguyen DT, et al. Bilayer tablets with sustained-release metformin and immediate-release sitagliptin: preparation and in vitro/in vivo evaluation. *Journal of Pharmaceutical Investigation*. 2021;51(5):579–586; doi: 10.1007/S40005-021-00533-Z/METRICS.

جسيمات نانوية من الفيبروين معدلة ببولي إيثيلين إيمين لإطلاق خاضع للتحكم كوسيلة محتملة للتوصيل الفموي للكوبرسيتين

فونغ تي إم .ها¹، ثانه ليتش نغوين²، نغوك ين نغوين²، نغوين ترونغ توان²، مانه كوان نغوين ٥، فونغ تي إم تران ثي بيش كوين ٩، دوي توان فام ٥٠٤

لقسم الكيمياء، كلية الصيدلة والتمريض، جامعة تاي دو، 68شارع تران تشيين، كان ثو 900000، فيتنام عقد المعلوم الطبيعية، جامعة كان ثو، الحرم الجامعي الثاني، شارع 3/2، كان ثو 900000، فيتنام ققسم الكيمياء التحليلية مراقبة جودة الأدوية، كلية الصيدلة، جامعة كان ثو للطب والصيدلة، 179شارع نغوين فان كو، كان ثو 900000، فيتنام الكيميائية، كلية الهندسة، جامعة كان ثو، الحرم الجامعي الثاني، شارع 3/2، كان ثو 900000، فيتنام

ملخص

تُعد المركبات متعددة الفينول فئة كبيرة من المركبات الكيميائية المستخدمة في تطبيقات طبية حيوية متنوعة. ومع ذلك، فإن هذه المركبات عرضة للتدهور، لا سيما ضمن بيئات الأس الهيدروجيني المتباينة في الجهاز الهضمي، مما يعيق استخدامها في الإعطاء الفموي. لذلك، يهدف هذا العمل إلى تطوير جسيمات نانوية من الفيبروين ((PNP) وجسيمات فيبروين معدلة ببولي إيثيلين إيمين ((HPEI-FNP) الحماية وتوصيل الكويرسيتين ((QC) فمويًا، باعتباره نموذجًا للمركبات متعددة الفينول. تم تحضير الجسيمات باستخدام طريقتين مختلفتين: الامتزاز والتكثيف المشترك. أظهرت الصيغتان خصائص فيزيائية حكيميائية مناسبة للإعطاء الفموي، بما في ذلك أحجام نانوية (حوالي 700 نانومتر لـ PPI-FNP-QC) توزيع حجمي ضيق (مؤشر تعددية النشت < 3.0)، إمكانات زيتا قابلة للتعديل (حوالي -20 مللي فولت لـ PPI-FNP-QC)، زيادة ذوبانية الكويرسيتين في الماء (حوالي -20 مللي فولت لـ PPI-FNP-QC)، زيادة ذوبانية الكويرسيتين في الماء بمقدار 2-3 مرات، وتفاعلات كيميائية ملحوظة (روابط هيدروجينية وتفاعلات أيونية) بين QC والفيبروين/ PEI-FNP-QC على ذلك، وبناءً على عملية التحضير وتركيب الجسيمات، أظهرت الجسيمات كفاءات احتواء معتدلة للكويرسيتين (35%)، وأسطحًا ناعمة أو خشنة، وامتصاصًا سريعًا للدواء يتبع نماذج تشمل متساوي حرارة لانغموير ودوبينين تمكنت من حماية إلى حركية من الدرجة الثانية الزائفة. المثير للاهتمام أن الجسيمات، في بيئة فموية محاكية، تمكنت من حماية QC في الظروف المعدية عند PH 1.2 بمعدلات يمكن التحكم بها من خلال تعديل طرق التحضير ولموفي قل من 20%، مع استمرار إطلاقه في الأمعاء عند PH 6.8 وكانون PPI-FNP إمكانات كبيرة كنظم توصيل دوائية خاضعة للتحكم للإعطاء الفموي للمركبات متعددة الفينول. من PN وPPI-FNP وPEI-FNP من PNP وPEI-FNP من PNP وPEI-FNP متعددة الفينول.

الكلمات الدالة: الفيبروين؛ بولى إيثيلين إيمين؛ الجسيمات النانوية؛ الكويرسيتين؛ التوصيل الفموي.

pdtoan@ctu.edu.vn

تاريخ استلام البحث 2024/08/01 وتاريخ قبوله للنشر 2024/09/21.

^{*} المؤلف المراسل: دوي توان فام